

## Bose-Einstein Condensation at a Helium Surface

E. W. Draeger\* and D. M. Ceperley

*Department of Physics and National Center for Supercomputing Applications, University of Illinois–Urbana-Champaign, Urbana, Illinois 61801*

(Received 8 January 2002; published 13 June 2002)

A path integral Monte Carlo method was used to calculate the Bose-Einstein condensate fraction at the surface of a helium film at  $T = 0.77$  K, as a function of density. Moving from the center of the slab to the surface, the condensate fraction was found to initially increase with decreasing density to a maximum value of 0.9 before decreasing. Long wavelength density correlations were observed in the static structure factor at the surface of the slab. Finally, a surface dispersion relation was calculated from imaginary-time density-density correlations.

DOI: 10.1103/PhysRevLett.89.015301

PACS numbers: 67.40.-w, 03.75.Fi, 67.57.Jj

It has been suggested [1] that the condensate fraction in the low density region near a  $^4\text{He}$  surface is significantly larger than the value in bulk helium of 0.1 [2]. Variational Monte Carlo (VMC) simulations by Lewart and Pandharipande [3] of small ( $N = 70$ )  $^4\text{He}$  droplets using a Jastrow one-body (JOB) trial wave function give evidence for a condensate fraction which approaches unity as the density goes to zero in the helium surface. However, subsequent calculations by Galli and Reatto [4] have shown that the condensate fraction throughout a helium surface computed using VMC is highly sensitive to the choice of trial wave function. They found that calculations performed using a shadow wave function with a glue term (G-SWF) have enhanced density-density correlations at long wavelengths [5], and a maximum condensate fraction of only 0.5. A helium surface with significant ripplon excitations is expected to have a lower condensate fraction compared with a surface which is flat, since the ripplons will couple velocities in the transverse directions above the surface. Quantum evaporation experiments [6] can be interpreted as providing evidence of an enhanced condensate fraction.

To avoid the problem of trial function bias and to include finite-temperature effects, we have used a path integral Monte Carlo (PIMC) method to calculate the density-density correlation functions and the condensate fraction at the surface of liquid  $^4\text{He}$ . We have also used imaginary-time correlation functions to calculate the dispersion relation of surface excitations in a free helium surface, and find good agreement with experimental thin film measurements.

Our simulation system consisted of  $^4\text{He}$  atoms, interacting pairwise with a very accurate potential [7]. Periodic boundary conditions were used with a box size and initial conditions chosen to favor a double-sided film oriented perpendicular to the  $z$  axis. To maintain a stable film and minimize finite size effects, we added an external potential determined from the long-ranged part of the interaction potential and the missing atoms from the other side of the slab, so that atoms on each of the two surfaces saw a po-

tential as if they were at the surface of a semi-infinite slab [8] (see Fig. 1).

Most of the calculations were performed with  $T = 0.77$  K, with an imaginary time step of  $\tau = 1/20$  K $^{-1}$ . We performed simulations of helium slabs containing  $N = 216$  and  $N = 432$  atoms, with dimensions  $(24 \times 24 \times 17)$  Å and  $(34 \times 34 \times 17)$  Å, respectively. Lower temperature calculations were also done to determine the temperature dependence.

In order to determine the extent to which ripplons are present in a free helium surface, we estimated density-density correlations at the surface [5] with the static structure factor defined as

$$S(k_{\parallel}; z, z') = \langle \rho_{k_{\parallel}}(z) \rho_{k_{\parallel}}(z') \rangle, \quad (1)$$

where  $\rho_k(z) \equiv 1/\sqrt{N(z)} \sum_i e^{i\mathbf{k}\cdot\mathbf{r}_i} \delta(z_i - z)$ ,  $N(z)$  is the number of particles in the bin at position  $z$ , and  $k_{\parallel}$  is the wave vector parallel to the surface. This measures the correlation between density fluctuations at vertical positions  $z$  and  $z'$ .

Figure 2 shows  $S(k_{\parallel}, z, z)$  curves as a function of density  $\rho(z)$ . Each curve is the average of both sides of

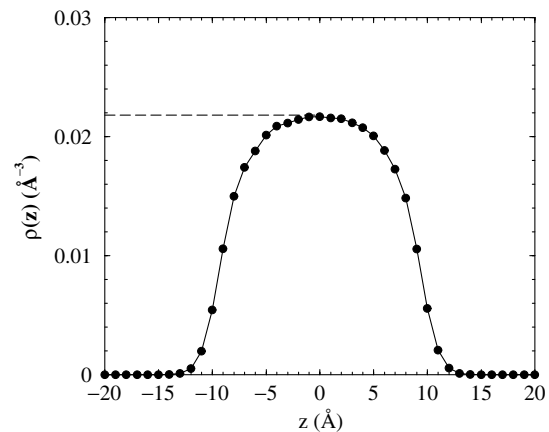


FIG. 1. PIMC density distribution, for an  $N = 432$ ,  $T = 0.77$  K semi-infinite  $^4\text{He}$  slab. The  $N = 216$  results are indistinguishable. The dashed line shows the effective helium density felt by atoms at  $z > 0$ .

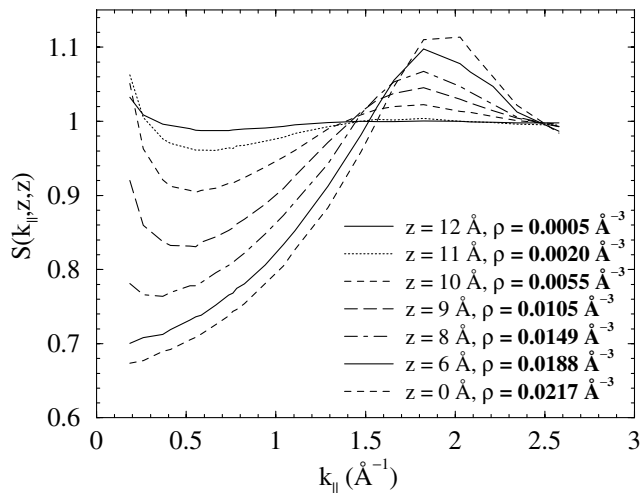


FIG. 2.  $S(k_{\parallel}, z, z)$  vs  $k_{\parallel}$  throughout the surface region in an  $N = 432$ ,  $T = 0.77$  K slab, calculated with PIMC.

the slab of eight identical simulations (a total of  $8 \times 10^5$  Monte Carlo passes). At  $T = 0.77$  K, for densities of  $\rho(z) = 0.015 \text{ \AA}^{-3}$  and below, there is a small enhancement of long-wavelength density-density correlations at  $k_{\parallel} = 2\pi/L = 0.18 \text{ \AA}^{-1}$ , which is evidence for riplons. However, the curves are closer to the VMC calculations of Galli and Reatto, which used a JOB trial wave function, than those which used the G-SWF form. This does not imply that the JOB trial wave function is well suited to representing an inhomogeneous helium system such as a helium slab, but rather the degree to which the G-SWF significantly overestimates the effect of riplons in a free helium surface. Calculations at  $N = 216$  and  $T = 0.77$  K agree with the  $N = 432$ ,  $T = 0.77$  K results of Fig. 2 within statistical error, indicating that finite-size effects are negligible. At  $T = 0.38$  K and  $N = 216$ , we find a measurable decrease in the long-wavelength correlations at  $k_{\parallel} = 2\pi/L = 0.26 \text{ \AA}^{-1}$ . Further studies are needed to establish the temperature dependence.

The excitation spectrum can be estimated with path integrals using imaginary-time correlation functions [9]. The dynamic structure factor is related to the imaginary-time density-density correlation function by

$$F(\mathbf{k}, t) = \int_{-\infty}^{\infty} d\omega e^{-t\omega} S(\mathbf{k}, \omega) \quad (2)$$

$$= \frac{1}{N} \langle \rho_{\mathbf{k}}(t) \rho_{\mathbf{k}}(0) \rangle. \quad (3)$$

To select out the excitations at the free surface, we want to calculate the imaginary-time correlation function of propagating surface modes. Saam [10] proposed that the lowest quantized hydrodynamic mode (capillary wave) at a free helium surface will have the form

$$\phi_{k0}(\mathbf{r}, t) = \phi_{k0}(z) e^{i\mathbf{k} \cdot \mathbf{r}_{\parallel}} e^{-i\omega_{k0}t}, \quad (4)$$

where

$$\phi_{k0}(z) \propto e^{-\kappa(k)z}, \quad (5)$$

and the decay constant  $\kappa(k)$  is defined as

$$\kappa(k) = -b_k + (k^2 + b_k^2)^{1/2}, \quad (6)$$

$$b_k \equiv \frac{\sigma_0 k^2}{2\rho_0 s^2}, \quad (7)$$

where  $\sigma_0$  is the zero-temperature surface tension,  $\rho_0$  is the bulk density, and  $s$  is the zero-temperature sound velocity. To calculate the dispersion relations for excitations of this form, we use  $\tilde{\rho}_{\mathbf{k}}$  in Eq. (3), defined as

$$\tilde{\rho}_{\mathbf{k}} = \sum_i e^{i\mathbf{k}_{\parallel} \cdot \mathbf{r}_{i\parallel}} \phi_k(z_i), \quad (8)$$

where

$$\phi_k(z) = \begin{cases} e^{-\kappa(k)(z-z_c)} & \text{if } z \leq z_c \\ 1 & \text{if } z > z_c \end{cases}, \quad (9)$$

and  $\kappa(k)$  is defined by Eq. (6). We defined  $z_c$  as the point in the surface at which the average density was equal to 10% of the bulk density. Tests have shown that the results are not sensitive to the value of  $z_c$ .

Extracting the dynamic structure factor by inverting Eq. (2) is ill-conditioned in the presence of statistical noise. It has been shown [11] that a maximum entropy method greatly increases the numerical stability. In the maximum entropy method,  $S(k, \omega)$  is calculated by minimizing the function,

$$\mathcal{F}(S, \alpha) = \frac{e^{-(1/2)Q(S)}}{Z_Q} \frac{e^{\alpha \zeta(S)}}{Z_{\zeta}}, \quad (10)$$

where  $Q(S)$  is the ‘‘likelihood’’ of the PIMC data given an  $S$ , and  $\zeta(S)$  is the entropy of a given  $S(k, \omega)$  defined with respect to some default model, with  $\alpha$  an adjustable parameter (also optimized).

The dispersion energy for a given value of  $k$  can be determined from the position of the maximum value of  $S(k, \omega)$ . Boninsegni and Ceperley [12] found that the position of the main  $S(k, \omega)$  peaks for liquid helium agree quite well with experiment, despite significant broadening of the excitation spectrum caused by the maximum entropy procedure. The dispersion energy of the surface excitations as estimated using this procedure are shown in Fig. 3. The two lowest data points, at  $k < 0.5 \text{ \AA}^{-1}$ , had significant fitting error and are only qualitatively reliable. Otherwise, we see excellent agreement with the experimental thin film data of Lauter *et al.* [13], including the curvature of the ripplon branch toward the roton minimum, proposed as evidence for roton-riplon hybridization [15,16].

We define the condensate fraction in the slab geometry by the fraction of atoms at a given value of  $z$  having precisely  $k_{\parallel} = 0$ . (Because  $[k_{\parallel}, z] = 0$ , we can measure the momentum parallel to the surface simultaneously with the  $z$  position.) The momentum distribution at a distance  $z_0$  from the center of the slab is given by

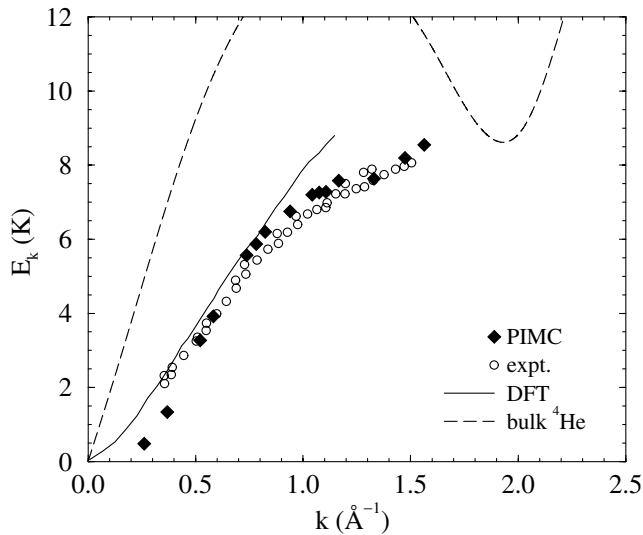


FIG. 3. Dispersion relation of free surface excitations. The results calculated from PIMC and maximum-entropy inversion (filled diamonds) for an  $N = 216$ ,  $T = 0.77$  K  $^4\text{He}$  slab are compared with the experimental thin film data (open circles) of Lauter *et al.* [13] and the density functional theory results (solid line) of Lastri *et al.* [14]. Also shown is the dispersion relation of bulk  $^4\text{He}$  at saturated vapor pressure (dashed line).

$$n_{\mathbf{k}_{\parallel}}(z_0) = \frac{1}{(2\pi)^2} \int d\mathbf{r}_{\parallel} e^{-i\mathbf{k}_{\parallel} \cdot \mathbf{r}_{\parallel}} n(\mathbf{r}_{\parallel}; z_0), \quad (11)$$

where the off-diagonal single particle density matrix is

$$n(\mathbf{r}; z) = \frac{1}{\rho} \langle z | Z \int d\mathbf{r}_1 \cdots d\mathbf{r}_N \times \rho(\mathbf{r}_1, \mathbf{r}_2, \dots, \mathbf{r}_N, \mathbf{r}_1 + \mathbf{r}, \mathbf{r}_2, \dots, \mathbf{r}_N; \beta), \quad (12)$$

where  $\rho$  is the many-body density matrix, and  $Z = \text{Tr}(\rho)$  is the partition function. This function can be calculated from PIMC [17] by performing simulations with a single open path. We fix the end points of the open path at  $z = z_0$ , and calculate the distribution of end-to-end distance  $n(r_{\parallel}; z_0)$ . The condensate fraction at a given point in the surface is

$$n_0(z_0) = \frac{n(r_{\parallel} \rightarrow \infty; z_0)}{n(r_{\parallel} \rightarrow 0; z_0)}. \quad (13)$$

Using PIMC, we calculated  $n(r_{\parallel}, z)$  throughout the slab (see Fig. 4). Nonlinear least-squares fitting was used in the region of  $r_{\parallel} < 1.5$  Å to get an estimate of  $n(r_{\parallel} = 0, z)$ , and  $n(r_{\parallel} \rightarrow \infty, z)$  was calculated by averaging over the region at large  $r_{\parallel}$ , where  $n(r_{\parallel}, z)$  is flat. At the lowest densities, it is not clear whether  $n(r)$  has reached its asymptotic limit within the finite simulation box. Thus, for  $N = 216$  at densities below  $\rho(z) = 0.001$  Å $^{-3}$ , our results are upper bounds to the condensate fraction. Even with  $N = 432$  atoms, finite-size effects may be significant at the lowest densities, due to the omission of long-wavelength ripples, as evidenced by the slow decay of  $n(r)$ .

The condensate fraction  $n_0(z)$  is plotted as a function of average density  $\rho(z)$  in Fig. 5, for both  $N = 216$  and  $N =$

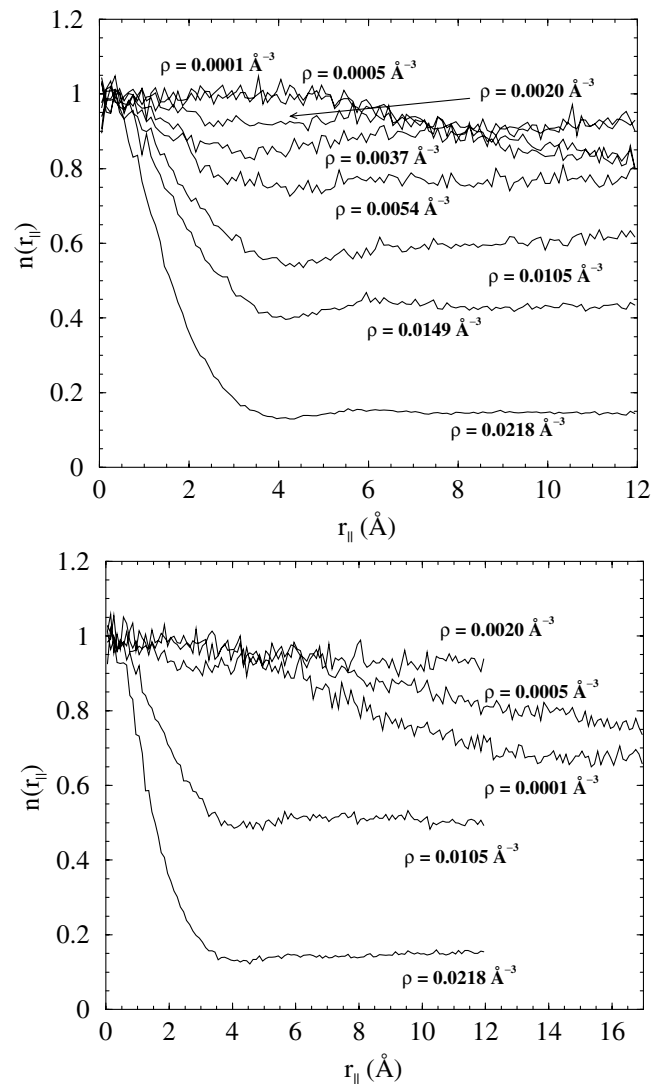


FIG. 4.  $n(r_{\parallel}, z)$  vs  $r_{\parallel}$ , throughout the surface region of  $N = 216$  (top) and  $N = 432$  (bottom)  $^4\text{He}$  slabs at  $T = 0.77$  K, calculated with PIMC. The slab dimensions were  $(24 \times 24 \times 17)$  Å and  $(34 \times 34 \times 17)$  Å, respectively. Density labels correspond to  $z = 0, 8, 9, 10, 10.5, 11, 12$ , and  $13$  Å for  $N = 216$ , and  $z = 0, 9, 11, 12, 13$  Å for  $N = 432$ .

432 helium slabs. As one moves through the surface, the condensate fraction initially increases with decreasing density, due to the decreased zero-point motion from helium-helium interactions, reaching a maximum value of 0.93(3) at  $\rho(z) = 0.002$  Å $^{-3}$ . As the average density decreases below this point, the condensate fraction begins to decrease, further evidence for correlated density fluctuations due to ripples at the surface. This is in qualitative agreement with the G-SWF VMC calculations of Galli and Reatto. However, the G-SWF trial wave function significantly overestimates the degree to which ripples are present in the surface.

We find that the probability of a given atom belonging to a long exchange cycle does not change if that atom is located above the surface. Hence, the density fluctuations

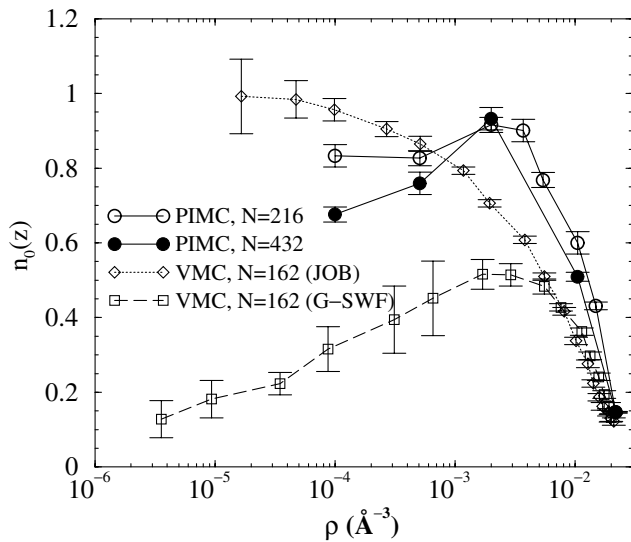


FIG. 5. Condensate fraction vs density throughout the surface region of a  $T = 0.77$  K  $^4\text{He}$  slab, calculated from the  $n(r_{\parallel}, z)$  curves in Fig. 4. Also shown are the VMC calculations of Galli and Reatto.

pulling atoms above the surface are accompanied by other (exchanging) atoms, in qualitative agreement with the ripplon model. But there is also present an appreciable fraction ( $\approx 30\%$ ) of nonexchanging atoms, possibly a result of finite temperature excitations.

We have presented PIMC calculations of the density-density correlation functions and condensate fraction at a free helium surface. These results support the model of a free helium surface with ripples, in which the condensate fraction reaches a maximum at an intermediate density in the liquid-vacuum interface, before decreasing at lower densities. Experimental probes of the surface will indeed see an enhanced condensate fraction as proposed by Griffin and Stringari [1].

This research was carried out on the Origin 2000 at the National Center for Supercomputing Applications and

the IBM cluster at the Materials Computation Center, and was supported by the NASA Microgravity Research Division, Fundamental Physics Program. This work was also performed under the auspices of the U.S. Department of Energy by University of California Lawrence Livermore National Laboratory under Contract No. W-7405-Eng-48.

\*Present address: Lawrence Livermore National Laboratory, 7000 East Avenue, L-415, Livermore, CA 94550.

- [1] A. Griffin and S. Stringari, *Phys. Rev. Lett.* **76**, 259 (1996).
- [2] O. Penrose and L. Onsager, *Phys. Rev.* **104**, 576 (1956).
- [3] D. S. Lewart, V. R. Pandharipande, and S. C. Pieper, *Phys. Rev. B* **37**, 4950 (1988).
- [4] D. E. Galli and L. Reatto, *J. Low Temp. Phys.* **113**, 223 (1998).
- [5] D. E. Galli and L. Reatto, *J. Phys. Condens. Matter* **12**, 6009 (2000).
- [6] A. F. G. Wyatt, *Nature (London)* **391**, 56 (1998).
- [7] R. A. Aziz, A. R. Janzen, and M. R. Moldover, *Phys. Rev. Lett.* **74**, 1586 (1995).
- [8] M. Wagner and D. M. Ceperley, *J. Low Temp. Phys.* **94**, 161 (1994).
- [9] D. M. Ceperley, *Rev. Mod. Phys.* **67**, 279 (1995).
- [10] W. F. Saam, *Phys. Rev. B* **12**, 163 (1975).
- [11] J. E. Gubernatis, M. Jarrell, R. N. Silver, and D. S. Sivia, *Phys. Rev. B* **44**, 6011 (1991).
- [12] M. Boninsegni and D. M. Ceperley, *J. Low Temp. Phys.* **104**, 339 (1996).
- [13] H. J. Lauter, H. Godfrin, V. L. P. Frank, and P. Leiderer, *Phys. Rev. Lett.* **68**, 2484 (1992).
- [14] A. Latri, F. Dalfovo, L. Pitaevskii, and S. Stringari, *J. Low Temp. Phys.* **98**, 227 (1995).
- [15] E. Krotscheck, S. Stringari, and J. Treiner, *Phys. Rev. B* **35**, 4754 (1987).
- [16] L. Pitaevskii and S. Stringari, *Phys. Rev. B* **45**, 13 133 (1992).
- [17] D. M. Ceperley and E. L. Pollack, *Can. J. Phys.* **65**, 1416 (1987).